Pure appl. geophys. (2007)
DOI 10.1007/s00024-007-0219-2

Pure and Applied Geophysics

Seasonal Sensitivity on COBEL-ISBA Local Forecast System for Fog and Low Clouds

Stevie Roquelaure and Thierry Bergot

Abstract—Skillful low visibility forecasts are essential for air-traffic managers to effectively regulate traffic and to optimize air-traffic control at international airports. For this purpose, the COBEL-ISBA local numerical forecast system has been implemented at Paris CDG international airport. This local approach is robust owing to the assimilation of detailed local observations. However, even with dedicated observations and initialization, uncertainties remain in both initial conditions and mesoscale forcings. The goal of the research presented here is to address the sensitivity of COBEL-ISBA forecast to initial conditions and mesoscale forcings during the winter season 2002–2003. The main sources of uncertainty of COBEL-ISBA input parameters have been estimated and the evaluation of parameter uncertainty on the forecasts has been studied. A budget strategy is applied during the winter season to quantify COBEL-ISBA sensitivity. This study is the first step toward building a local ensemble prediction system based on COBEL-ISBA. The conclusions of this work point out the potential for COBEL-ISBA ensemble forecasting and quantify sources of uncertainty that lead to dispersion.

Key words: Local numerical forecast system, fog and low clouds, seasonal sensitivity, initial conditions and mesoscale forcings uncertainties, forecast dispersion, local ensemble prediction system.

1. Introduction

Accurate prediction of fog and low clouds is one of the main issues related to improving air-traffic management and safety. At Paris Charles de Gaulle (CdG) international airport, adverse ceiling and visibility conditions (visibility under 600 m and ceiling below 60 m) lead to the application of Low Visibility Procedures (LVP). Under these conditions, the airport take-off/landing efficiency is reduced by a factor of 2, causing aircraft delays. In this context, accurate short-term forecasts of LVP conditions are considered to be a priority by airport authorities.

Unfortunately, current operational Numerical Weather Prediction (NWP) models are not able to provide detailed information due to their lack of both vertical and horizontal resolutions with respect to the typical length scale of fog. However, owing to higher vertical resolution and more detailed physics than 3D

Météo-France, Centre National de Recherches Météorologiques, CNRM/GMME, 42 Av Coriolis, F-31057 Toulouse Cedex, France. E-mail: stevie.roquelaure@cnrm.meteo.fr

NWPs, one-dimensional modeling is an attractive alternative (e.g., MUSSON-GENON, 1986; DUYNKERKE, 1991; BERGOT and GUÉDALIA, 1994). This 1-D approach to forecast the fog and low cloud life cycle is currently used operationally at San Francisco airport (CLARK, 2002) and at CdG airport (BERGOT *et al.*, 2005). The same kind of strategy is tested in the northeast corridor within the framework of the US Federal Aviation Administration ceiling and visibility project (HERZEGH *et al.*, 2002).

The numerical prediction method used at CdG (see BERGOT, *this issue* for more details) includes:

- Specific observations from a 30 m meteorological tower (atmospheric temperature and humidity, shortwave and longwave radiation fluxes) and soil measurements;
- the mesoscale forcings (mesoscale advection, geostrophic wind and cloud cover) are evaluated from the Météo-France operational NWP model Aladin (see http://www.cnrm.meteo.fr/aladin/);
- a local assimilation scheme is used to construct initial conditions, based on a 1-D-var assimilation scheme together with a fog and low cloud specific initialization;
- the 1-D high resolution COBEL-COde de Brouillard à l'Echelle Locale (Local scale fog code) atmospheric model (BERGOT, 1993; BERGOT and GUÉDALIA, 1994) coupled with the multilayer surface-vegetation-atmosphere transfer scheme ISBA-Interaction Soil Biosphere Atmosphere (BOONE *et al.*, 2000; BOONE, 2000).

BERGOT (*this issue*) documented the conditions when the local approach should be useful. However, a finer understanding of the limits of predictability for the specific case of fog and low clouds also needs to be performed. Which is the main goal of the current study. Under the hypothesis of a ''perfect model'', the uncertainty of forecasts made with the Cobel-Isba numerical system arises from uncertainty caused by two distinct sources of errors, namely, from errors in the specification of the initial conditions, as well as errors in the specification of the mesoscale forcings. Here the focus is on very short-term forecasts and attention is restricted to a perfect model situation. The influence of model errors will be studied in future work. This is the first step toward building a local 1-D Ensemble Prediction System (L-EPS) based on the COBEL-ISBA model.

In the first stage, the input uncertainties have been evaluated following the spatial and temporal variability of input data. The methodology and the uncertainties regarding input parameters will be discussed in section 2. In the second stage, the impact of input uncertainties for COBEL-ISBA LVP forecasts is examined. A key aspect of this study is to assess the input uncertainty impacts on the LVP forecast in order to evaluate the dispersion of Cobel-Isba forecasts, and also to obtain insights on how to build an efficient L-EPS. Usually, 1-D studies focus on selected cases and do not give a global overview of input uncertainty impacts. Here, the problem is examined from a seasonal point of view by running the local prediction system for the winter season 2002–2003 with a three-hour data assimilation frequency. This approach permits the evaluation of the overall impact of the main input uncertainties for the

prediction of foggy conditions at CdG. In section 3, these results are summarized by focusing on the forecast scores during the winter for both initial condition and mesoscale forcing uncertainties. And finally, section 4 concludes with a discussion on how these results could be used to build a local ensemble prediction system.

2. Estimation of Uncertainties for Input Parameters

2.1. Mesoscale Forcing Uncertainties

2.1.1. Methodology

The mesoscale forcing is provided by the operational NWP model Aladin (http://www.cnrm.meteo.fr/aladin/). Three different forcing terms are evaluated: horizontal advections, geostrophic wind and cloud cover. Aladin has a 10 km horizontal resolution. However, even with this resolution unresolved scales or errors in the mesoscale initial conditions induce noticeable variability at the grid point and in the neighborhood of the study zone in time, revealing the model uncertainty (ROQUELAURE, 2004). Unfortunately, it is not possible to accurately define the uncertainties of the mesoscale forcing terms, for example by comparing with measurements. To overcome this difficulty, it is necessary to evaluate the uncertainties from the Aladin forecasts only.

The mesoscale forcing uncertainty computation is then based on the hypothesis that uncertainty is correlated with the variability of the NWP model. The model variability is assessed in both space and time. The spatial variability is evaluated by comparing the forecast over an area of 3×3 grid points. This area is representative of homogeneous surface conditions around the study area. Moreover, it is not possible to extend this homogeneous area due to the presence of urbanized areas in the south-west (Paris). The temporal variability is evaluated by comparing four Aladin runs (0, 6, 12 and 18 UTC) for the same verification time. This choice allows the comparison of short-term forecasts only. At the end of this process, the variability in both space and time is used to estimate the shape of the distribution of uncertainties.

2.1.2. Horizontal advection

The temperature and humidity advection are computed over 9 grid points using the spatio-temporal approach for uncertainty computation. Figures 1a and 1b show, respectively, the temperature and humidity advection uncertainty distributions on winter season 2002–2003 for the Aladin vertical levels below 1 km within the boundary layer. Both temperature and humidity advection distributions have a "V" symmetrical shape, which indicates a linear growth of the uncertainty along with the rise of the mean advection value. However, notice that for small advection intensities in terms of the absolute value (lower 0.1 $C.h^{-1}$ for temperature advection and lower than 0.05 $g.kg^{-1}.h^{-1}$ for humidity advection), the mean advections have the same

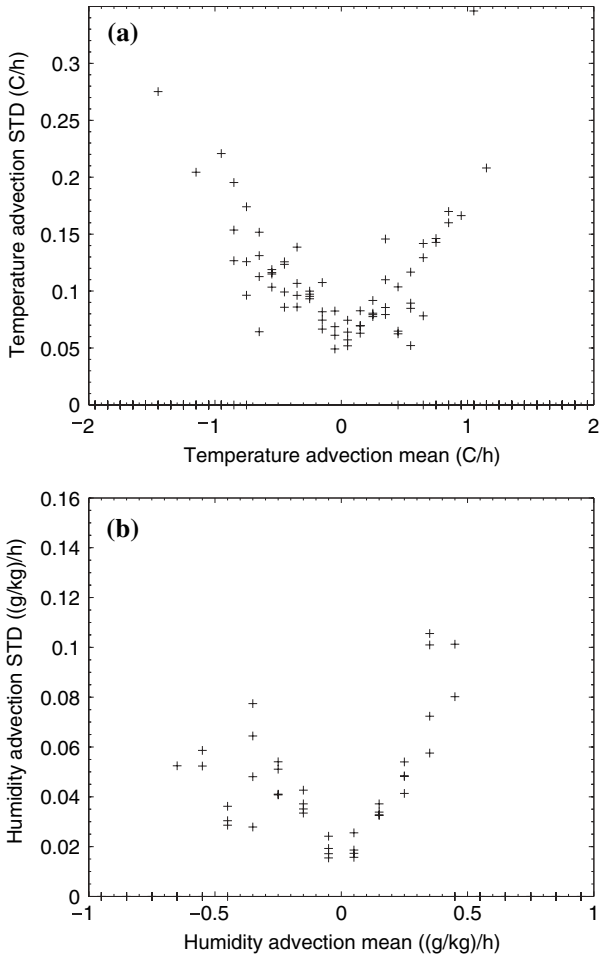

Figure 1
Aladin temperature (a) and humidity (b) advection uncertainty distributions for vertical levels below 1 km.

magnitude as the uncertainty. In radiative fog events frequently observed in CdG, the magnitude of the advections is relatively small (a fog event associated with weak winds). In these situations, advection uncertainty is as important as the mean advection. For conditions representative of higher advection values, the order of magnitude of the uncertainty increases weakly as the advection mean values increase. For temperature advection values over 0.2 $C.h^{-1}$ and humidity advection values over 0.05 $g.kg^{-1}.h^{-1}$, uncertainty is less than 40% of the advection.

2.1.3. Geostrophic wind

The geostrophic wind is computed from the horizontal pressure gradient and it is computed over a 100×100 km^2 area (see BERGOT *et al.*, 2005 for more details).

Figure 2 presents the geostrophic wind uncertainty as a function of the mean geostrophic wind for the winter season 2002–2003 and for vertical levels below 1 km. The evolution of the geostrophic mean wind uncertainty is almost linear for wind speeds below 15 m/s. In the case of fog, wind strength is generally below 6 m/s and even below 2 m/s in case of radiative fog, and the wind uncertainty is about 1 m/s.

2.1.4. Cloud cover

Current NWP models do not accurately forecast thin clouds or boundary layer clouds (e.g., stratocumulus). However, the appearance and the life cycle of a fog layer is very sensitive to the presence of cloud cover. Unfortunately, the spatial and temporal variation of the Aladin cloud cover are very small and it is not possible to estimate the cloud cover uncertainty by using the previously mentioned method (the cloud cover uncertainty mainly comes from approximations made in physical parameterization schemes). Two extreme hypotheses have been tested: a clear sky hypothesis and a persistence hypothesis. The persistence hypothesis is based on the assumption that the observed cloud cover is maintained during the 12 hours of the simulation, while the clear sky hypothesis assures that the sky remains clear during this period. An intermediate situation is also possible, by using the Aladin cloud cover forecasts. These three simulation cycles have been performed to quantify the cloud cover impact. Comparisons between 2 m downward longwave observations and COBEL-ISBA radiative fluxes using the clear sky hypothesis reveal a significant bias and standard deviation of the downward longwave fluxes (bias = -16.6 W/m^2, and std = 25 W/m^2). The Aladin and persistence cycles have a weaker bias for the 2 m longwave radiative fluxes (the bias for Aladin cycle = -6.4 W/m^2, and the bias

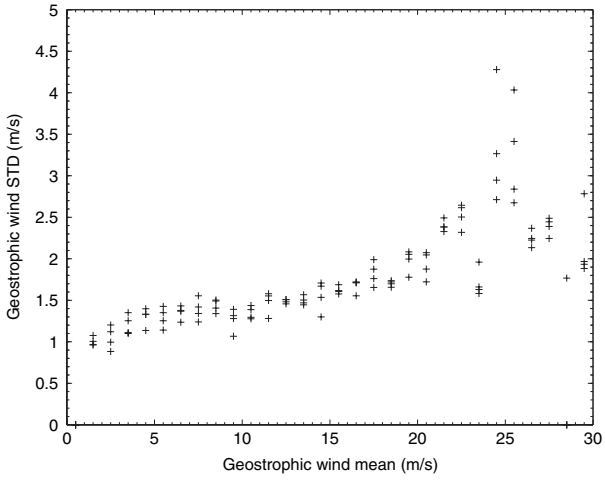

Figure 2
Aladin geostrophic wind uncertainty distribution for vertical levels below 1 km.

for persistence cycle = −2.3 W/m^2) in addition to a lower standard deviation (std for Aladin cycle = 19.8 W/m^2 and std for persistence cycle = 14.3 W/m^2).

2.2. Initial Condition Uncertainties

Initial conditions must be specified for both atmosphere and soil. Soil temperature and moisture profiles are estimated from on-site observations. The COBEL-ISBA analysis is based upon local observations, a guess field (which is the previous COBEL-ISBA forecast) and forecast profiles from NWP model Aladin. The 1-D variational assimilation scheme makes use of all this information to produce the best analysis possible. Through the 1-D variational assimilation process, observations are prevailing in the surface boundary layer. Above the surface boundary layer, as no observations are available, the COBEL guess issued from the previous forecast and the Aladin profile are combined. For more information on COBEL-ISBA data assimilation system, see BERGOT *et al.* (2005).

2.2.1. Atmospheric temperature and humidity profiles

Observations are the main information used to compute the atmospheric profiles in the surface boundary layer through the variational assimilation. Consequently, the low level temperature and humidity uncertainties are well represented by measurement uncertainties for both the temperature and the humidity. These measurement uncertainties are estimated at 0.2 degree Celcius for temperature and 0.2 g.kg^{-1} for humidity (see MARZOUKI, 2005). For the upper part of the boundary layer, the analysis follows the COBEL guess and the Aladin profiles. In practice, in order to compute uncertainties for upper atmospheric layers, we used the spatio-temporal method described in section 2.1.1. The estimated uncertainties are 0.6 degree Celcius for temperature and 0.5 g.kg^{-1} for humidity. A smooth linear interpolation is applied between the surface boundary layer where the measurement uncertainties prevail and the upper part of the boundary layer where Aladin uncertainties dominate.

2.2.2. Fog and stratus initialization

The fog/stratus initialization of COBEL-ISBA is based on an iterative method (BERGOT *et al.*, 2005). The depth of the cloud layer is determined by minimizing the radiation flux divergence between 2 m and 45 m (the two levels of radiative measurements). If the fog or low clouds are above the upper level of the radiative measurements (45 m), the fog depth is estimated by minimizing the errors of the radiative fluxes at the ground. CARRER (2003) has shown that the uncertainty is on the order of +/− 1 Cobel grid point for very low clouds (cloud top below 45 m). On the other hand, for events with higher cloud tops, uncertainty is more significant and diagnostics done by CARRER (2003) reveal that the uncertainty is on the order of +/− 2 Cobel grid points.

The liquid water content (LWC) uncertainty impact on LVP forecasts is addressed when fog (or stratus) is detected and initialized. Studies by MEYER *et al.* (1986) and WALMSLEY *et al.* (1999) have shown that LWC in fog ranges between 0.08 and 0.5 g.kg^{-1}. Here the goal is to analyze the impact of the small change of LWC in the cloud initialization. A 0.05 g.kg^{-1} liquid water uncertainty is then added (or removed) to the cloud reference liquid water content.

2.2.3. Soil temperature and moisture initialization

Soil temperature and moisture uncertainties are estimated from the accuracy of the measurements. Observed soil temperature and humidity variability during the winter are used to estimate soil vertical profile uncertainties for temperature and humidity. The maximum variability observed at each level is used as an estimate of uncertainty. Soil temperature uncertainty is constant at 0.1 degree Celcius up to −30 cm, and increases linearly up to 1 degree Celcius close to the surface. Soil humidity uncertainty is also constant up to −30 cm at 0.01 g.kg^{-1}, and increases linearly up to 0.025 g.kg^{-1} near the surface.

3. Forecast Sensitivity

3.1. Statistics Used to Perform Diagnostics

Numerous COBEL-ISBA simulations have been performed continuously for the winter season 2002–2003 for each perturbed configuration. A sensitivity study is conducted by comparing three different cycles (in a perturbed cycle, only the studied parameter is perturbed): the reference cycle (non perturbed), the cycle "+" (perturbed by adding the uncertainty), the cycle "−" (perturbed by subtracting the uncertainty).

The main statistical tools used to examine the quality of LVP forecasts (and the dispersion between perturbed cycles) are the Hit Rate (HR) and the False Alarm Rate (FAR). If a is the number of observed and forecasted events, b is the number of not observed and forecasted events, and c is the number of observed and not forecasted events, HR and FAR are defined by equations (1) and (2):

$$\mathrm{HR} = \frac{a}{a+c}, \tag{1}$$

$$\mathrm{FAR} = \frac{b}{a+b}. \tag{2}$$

The difference between the perturbed cycles scores (HR and FAR) is used. Uncertainty quantification is made by determining dispersion on LVP scores between the two perturbed cycles.

$$\mathrm{Dispersion} = \|S_{perturbed\_cycle+} - S_{perturbed\_cycle-}\| \tag{3}$$

where S can either represent HR or FAR at a particular forecast time during the 12 h simulation.

This study is designed to analyze initial conditions (IC) and mesoscale uncertainty impacts on the LVP forecast. However, uncertainty also has an indirect impact on thermodynamic parameters such as heat and humidity. Consequently, a heat and humidity budget strategy is applied to COBEL profiles to look at this question. IC and mesoscale perturbations act upon the 3-hour run needed to produce a guess field for the next assimilation. As a consequence, COBEL initial profiles are influenced by perturbations through the computation of the guess field (Fig. 3). Comparing the perturbed and the reference cycle budgets for each run during the winter season is an efficient way to quantify heat (or humidity) changes. Equation (4) gives the computation of the fraction R of heat (or humidity) gain (or loss) in the guess profiles due to uncertainty at time t for a perturbed cycle:

$$R = \frac{Q_{perturbed} - Q_{reference}}{Q_{reference}}, \tag{4}$$

where Q can either represent the heat or the humidity column balance. Subscripts refer to either the reference cycle or a perturbed cycle at time t. The mean and standard deviation of the R are computed in order to quantify the mean uncertainty impact and the variability of this impact on the winter period. Both scores are important in this context because sensitivity can be revealed by the variability of R coefficient and also by the mean value.

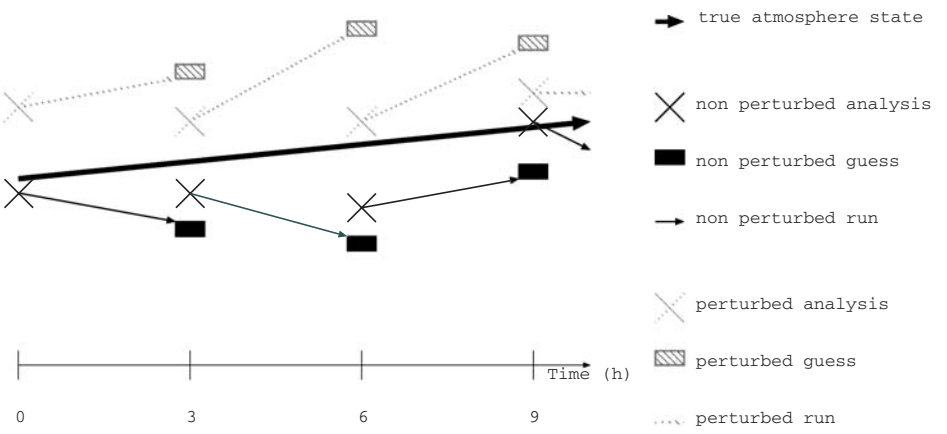

Figure 3
Schematic representation of perturbed cycles.

3.2. Forecast Sensitivity to Initial Conditions

The goal of this section is to evaluate the impact of initial condition uncertainties on LVP forecasts. The reference cycle and the perturbed cycles are done with the clear sky hypothesis (without cloud cover) and without advection.

3.2.1. Forecast sensitivity to atmospheric profiles uncertainties

The uncertainty previously estimated has been applied to the COBEL atmospheric profiles at the initial time. Tables 1 and 2 show that temperature uncertainty causes more dispersion for the LVP scores than humidity uncertainty. For humidity, dispersion is weak and almost constant during the runs (under 3%) for both HR and FAR, whereas dispersion reaches 15.5% for HR and 8% for FAR for the temperature at 9 h. The budget strategy results (Table 3) reveal that the atmospheric temperature uncertainty has an impact on both temperature and humidity in the guess atmospheric profile. For the warmer cycle, the mean heat change is 0.28% (std = 0.08%) and the mean humidity is 0.48% (std = 1.57%). This double impact can explain the higher dispersion made by temperature uncertainty. Actually, atmospheric humidity uncertainty has minimal impact on the heat balance. For example, mean impact of the moister cycle for the winter is very low (mean = −0.001% and std = 0.02%).

Figure 5 shows that the reference cycle scores (HR and FAR) do not necessarily lie between the perturbed cycles scores. Dispersion is asymmetric from the reference cycle. The colder cycle leads to similar scores as the reference cycle, but the warmer cycle gives better scores for both HR and FAR. This result suggests that there might be a cold bias in the atmospheric boundary layer profiles from the Aladin NWP model. The better results for both scores at most forecast times may be explained by the cold bias correction induced by the warm uncertainty applied for the atmospheric temperature profile.

Table 1

Hit Rate (HR) dispersion for perturbed cycles. Values of dispersion over 10% are in bold

$\|HR_{perturbed\_cycle+} - HR_{perturbed\_cycle-}\|$ (%)	Forecast time (hour)				
	1	3	6	9	12
Atmospheric temperature (initial condition)	0.0	2.3	9.4	**15.5**	2.4
Atmospheric humidity (initial condition)	2.9	2.3	2.4	0.0	2.4
Clouds depth (initial condition)	**17.6**	**23.2**	**28.9**	**24.3**	**19.5**
Clouds liquid water (initial condition)	**11.7**	**16.2**	4.6	**12.1**	9.7
Soil temperature (initial condition)	**20.5**	4.6	4.6	9.7	7.3
Soil moisture (initial condition)	8.7	0.0	2.4	2.5	0.0
Geostrophic wind (mesoscale forcing)	5.8	9.2	7.0	4.8	4.7
Cloud cover (mesoscale forcing)	5.9	2.3	4.7	4.8	7.3
Temperature advection (mesoscale forcing)	0.0	6.9	7.1	2.5	2.4
Humidity advection (mesoscale forcing)	**14.6**	**23.2**	**26.1**	**36.4**	**16.9**

Table 2

False Alarm Rate (FAR) dispersion for perturbed cycles. Values of dispersion over 10% are in bold

$\|(FAR_{perturbed\_cycle+} - FAR_{perturbed\_cycle-}\|$ (%)	Forecast time (hour)				
	1	3	6	9	12
Atmospheric temperature (initial condition)	3.3	1.4	6.4	8.0	0.5
Atmospheric humidity (initial condition)	1.9	0.1	0.7	2.9	0.2
Clouds depth (initial condition)	**23.9**	**14.4**	4.0	7.6	8.0
Clouds liquid water (initial condition)	6.2	2.4	1.7	4.9	3.4
Soil temperature (initial condition)	3.9	9.0	6.9	3.4	0.0
Soil moisture (initial condition)	0.4	0.0	1.4	1.3	0.4
Geostrophic wind (mesoscale forcing)	4.2	8.8	9.9	**13.5**	**11.0**
Cloud cover (mesoscale forcing)	7.7	4.9	5.2	5.9	4.3
Temperature advection (mesoscale forcing)	9.8	**10.3**	**10.3**	**13.5**	**14.1**
Humidity advection (mesoscale forcing)	7.7	**10.6**	9.1	7.4	**15.6**

Table 3

Heat and humidity mean changes in the atmospheric guess profile for the initial conditions cycle. Values over 0.2% for mean heat and mean humidity are in bold. Values over 0.1% and over 1% are in bold for the std of heat and the std of humidity, respectively

$\overline{R} = \overline{(Q_{perturbed} - Q_{reference})/Q_{reference}}$	Heat (%)		Humidity (%)	
	mean on cycle	std	mean on cycle	std
Temperature "+" (warmer)	**0.28**	0.08	**0.48**	**1.57**
Temperature "−" (colder)	−0.004	0.01	−0.009	0.38
Humidity "+" (moister)	0.001	0.02	**0.24**	0.50
Humidity "−" (drier)	−0.001	0.01	**−0.28**	0.49
Clouds depth "+" (deeper clouds)	−0.052	**0.136**	−0.18	**1.90**
Clouds depth "−" (thinner clouds)	0.021	0.071	**0.22**	**1.14**
Clouds liquid water "+" (heavier clouds)	0.008	0.068	0.15	**1.50**
Clouds liquid water "−" (lighter clouds)	−0.008	0.067	−0.009	**1.64**
Soil temperature "+" (warmer)	0.006	0.024	0.18	0.57
Soil temperature "−" (colder)	−0.005	0.031	**−0.23**	0.63
Soil humidity "+" (moister)	−0.001	0.018	0.02	0.56
Soil humidity "−" (drier)	0.004	0.024	−0.09	0.58

3.2.2. Forecast sensitivity to the low cloud initialization

For cloud initialization, perturbed cycles produce deeper or thiner clouds than the reference cycle. The first three simulation hours needed to compute the guess field are crucial. With different cloud properties, the vertical structure of the boundary layer could greatly change (Fig. 4). These changes are significant and evaluated with the budget strategy. Variability of the winter for humidity balance in the guess atmospheric profiles is high (1.9% for deeper clouds and 1.14% for thinner clouds). The heat balance variability is also significant (std = 0.136% for deeper clouds and

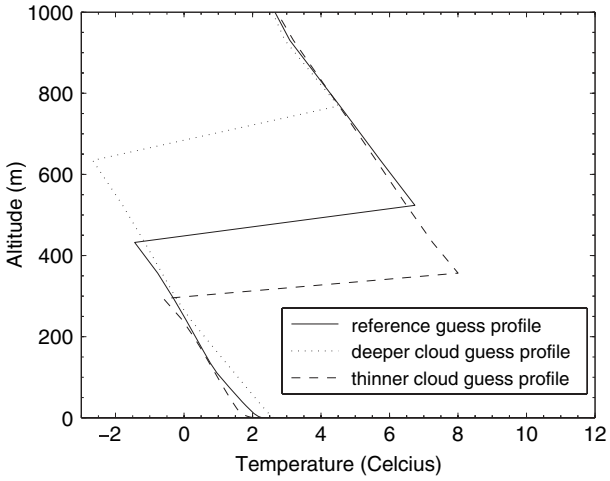

Figure 4
Guess used for the 12Z run of December 12th, 2002: The reference cycle (stratus initialised at 9Z, 90–430 m), deeper cloud cycle (stratus initialized at 9Z, 90–630 m) and thinner cloud cycle (stratus initialized at 9Z, 90–290 m).

0.071% for thinner clouds). As a consequence, the LVP score dispersion induced by the cloud depth uncertainty is significant (from 17.6% at 1 h to 28.9% at 6 h) for HR and (from 4% at 6 h to 23.9% at 1 h) for FAR.

Liquid water content (LWC) uncertainty leads indirectly to the same effects as for the fog/stratus depth initialization, by modifying the liquid water path. However, dispersion in that case is less significant than dispersion generated by a cloud depth uncertainty. Dispersion is below 17% for HR and below 7% for FAR.

3.2.3. Forecast sensitivity to soil profile uncertainties

Soil temperature uncertainty generates more LVP score dispersion than soil moisture uncertainty. Once again, the budget strategy (Table 3) shows that soil temperature uncertainty acts on both atmospheric thermodynamic parameters, whereas the soil moisture uncertainty acts essentially on the humidity balance. As a consequence, dispersion is over 4.5% for HR between perturbed soil temperature cycles. The dispersion is maximum at the beginning of the simulation (about 20%). For soil moisture perturbed cycles, the dispersion is under 3% for HR except for the beginning of the simulation, where dispersion is 8.7%. For FAR, the dispersion is under 2% between the perturbed soil moisture cycles, and between 0 to 9% for the perturbed soil temperature cycles.

3.3. Forecast Sensitivity to Mesoscale Forcings

1-D modeling allows a description of meteorological phenomenon at the local scale. Nevertheless, the mesoscale acts upon the local scale through the dynamical

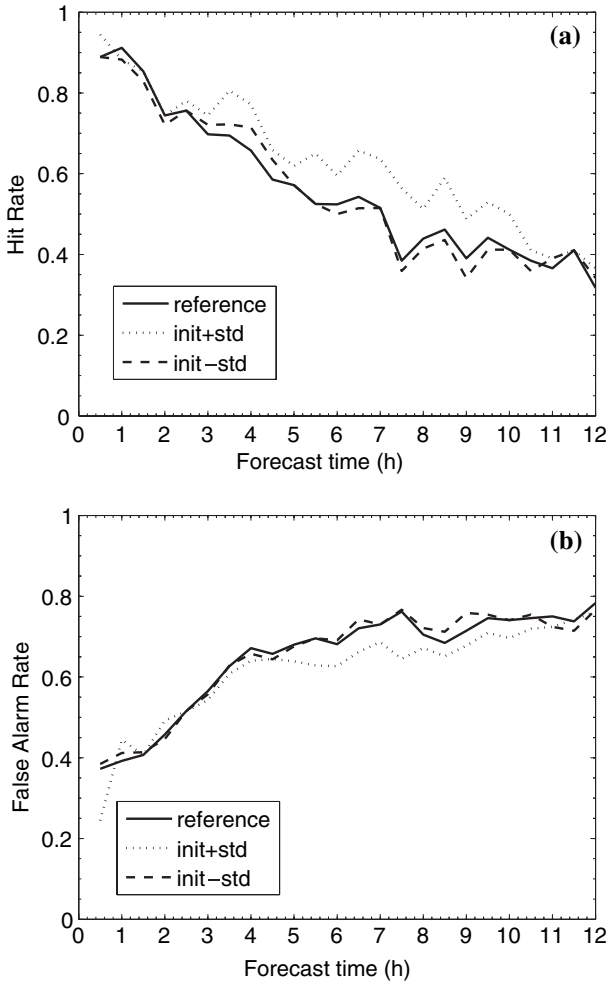

Figure 5
Hit rate (a) and false alarm rate (b) comparison for LVP forecast for the reference cycle, the perturbed atmospheric temperature cycles for winter season 2002–2003.

evolution of the atmosphere, and it is important to consider this interaction for fog and low cloud prediction. TURTON and BROWN (1987) and later BERGOT (1993) or BERGOT and GUÉDALIA (1994) have shown the importance of advection phenomenon in fog formation and evolution.

3.3.1. Forecast sensitivity to cloud cover

The impact of cloud cover is evaluated for three different cycles: the Aladin cloud cover cycle, which takes into account the cloud forcing based on Aladin forecasts, the

observed cloud cover persistence (constant cloud forcing during a COBEL run), and the clear sky cycle. Dispersion on LVP scores between cloud cover perturbed cycles is almost constant, around 5% for all forecast times for both HR and FAR. The budget strategy also reveals an important indirect impact on analyses through the guess field (Table 4). Variability for heat and humidity balances is high with values around 2.5% for humidity and 0.1% for heat balance with respect to both Aladin and the persistence cycles.

3.3.2. Forecast sensitivity to geostrophic wind

Geostrophic wind acts indirectly on the turbulence. The budget strategy shows that geostrophic wind uncertainties influence both heat and humidity balances during the computation of the guess field. The heat and humidity balance variability is moderate and is around 0.035% and 0.6% for the two perturbed cycles. Dispersion for HR is over 4.7%, and a higher spread is observed at 3 h and 6 h with values of 9.2 and 7%. Dispersion for FAR increases slowly during the 12 hours of simulation, beginning at 4.2% and ending close to 13%.

3.3.3. Forecast sensitivity to horizontal advection

First, it is of interest to note that advection forecasted by Aladin NWP models generally bring warmer and dryer air into the column compared to the cycle without advection (Figs. 6a and 6b). The budget strategy confirms a warm (mean = 0.05% and std = 0.32%) and dry (mean = −1.85% and std = 10.68%) mean advection effect during the winter (Table 4). Advection has a clear impact on the heat and humidity balances. Figure 7 shows the balances for each guess field and analysis during the winter. Variability is higher for the atmospheric profiles from the guess fields (10.68% for humidity and 0.32% for heat) than those from analyses for both thermodynamic variables because analyses are forced by observations in the assimilation process. The consequence of the dry and warm contribution of the advection is that the reference advection cycle damages the detection of LVP (HR) compared to the reference cycle (Fig. 8).

Temperature and humidity advection uncertainty impacts on LVP forecasts have been analyzed by separately perturbing temperature advection and humidity advection :

- The reference advection cycle (non perturbed),
- "AT + STD" by convention is a **colder advection** (perturbation of the temperature advection STD, without perturbation of the humidity advection (AQ)),
- "AT-STD" by convention is a **warmer advection** (perturbation of the temperature advection STD, without perturbation of the humidity advection (AQ)),
- "AQ + STD" by convention is a **drier advection** (perturbation of the humidity advection STD, without perturbation of the temperature advection (AT)),

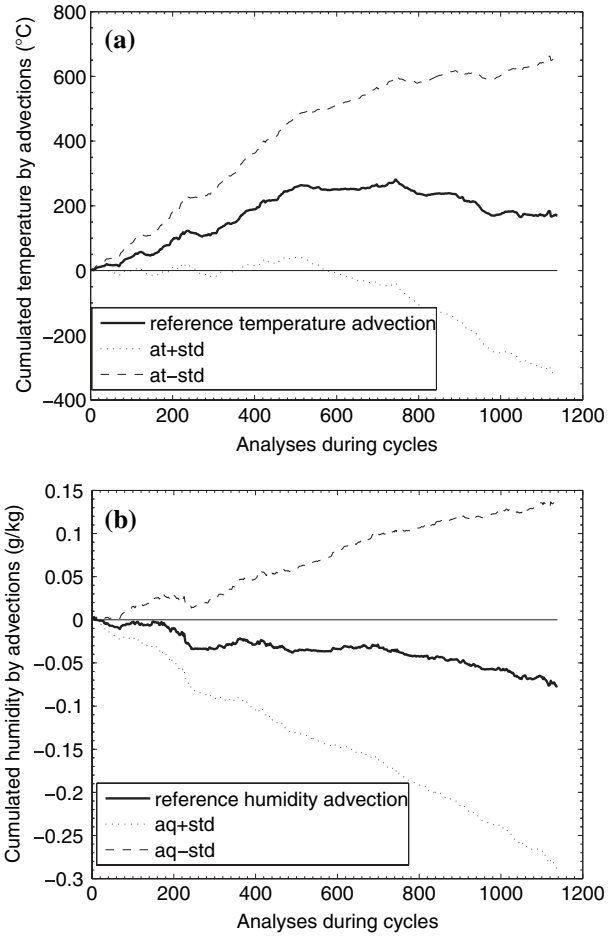

Figure 6
Cumulated (a) heat and (b) humidity during the winter season 2002–2003 for the advection cycles. Heat and humidity values are only computed from temperature and humidity advection inputs for COBEL.

- "AQ-STD" by convention is a **moister advection** (perturbation of the humidity advection STD, without perturbation of the temperature advection (AT)).

Figure 8a shows that the LVP score dispersion between temperature advection cycles is low during the first hours of the simulation. The HR spread becomes more important between 3 h and 9 h (7.1% at 6 h). Table 2 shows that the FAR dispersion is close to 10%, and it is almost constant during the 12 hours of simulation.

Both perturbed temperature advection cycles improve the HR score after two hours. The warmer cycle improves the score of the reference advection cycle, and the results become comparable to the reference cycle (without advection). This improvement, which is induced by warmer advection, pleads also in favor of a cold

Table 4

Same as Table 3 for mesoscale forcing cycles

$\overline{R} = \overline{(Q_{perturbed} - Q_{reference})/Q_{reference}}$	Heat (%)		Humidity (%)	
	mean on cycle	std	mean on cycle	std
Geostrophic wind "+" (stronger)	−0.005	0.038	0.05	0.63
Geostrophic wind "−" (lighter)	0.003	0.033	−0.17	0.77
Aladin cloud cover	0.022	**0.114**	**−0.28**	**2.53**
Observed cloud cover persistence	−0.009	0.077	**−0.93**	**2.45**
Advections without STD	0.051	**0.328**	**−1.85**	**10.68**
Temperature advection "+" (colder)	−0.14	0.05	**−0.23**	**1.02**
Temperature advection "−" (warmer)	0.14	0.05	**0.20**	0.94
Humidity advection "+" (drier)	−0.022	0.034	**−5.26**	**3.10**
Humidity advection "−" (moister)	0.025	0.054	**5.22**	**3.21**

bias in the Aladin profiles within the boundary layer (i.e., warmer atmospheric temperature uncertainty).

Figure 8b shows that dispersion between perturbed humidity advection cycles is very significant. Dispersion is low at the beginning of the simulation and increases significantly with time (14.6% at 1 h and 36.4% at 9 h for HR). On FAR, dispersion is close to 10% during the 12 hours of simulation. Compared to the reference advection cycle, asymmetry is observed between the dry and the moist cycles.

4. Summary and Perspectives

The prediction of low visibility conditions at airports is a challenge for forecasters. Previous studies have shown the potential of the COBEL-ISBA local numerical prediction system to fulfill this very specific need. The use of dedicated local observations and a local assimilation scheme to accurately initialize the COBEL-ISBA model has been conducive to improvements in fog and low cloud prediction (see BERGOT, *this issue*). However, despite these improvements, it is necessary to quantify the forecast quality. One way is to estimate the uncertainties with respect to the input parameters, such as initial conditions and mesoscale forcings, and to evaluate the impact of these uncertainties on fog and low cloud forecasts.

In this study, uncertainty distributions for both sources of error have been evaluated. Firstly, for mesoscale forcings, uncertainty has been estimated under the hypothesis that uncertainty is correlated with the "intrinsic" spatial and temporal variability of the Aladin NWP model. In conditions corresponding to fog and low clouds, it was found that the advection uncertainty is as important as the mean advection. Secondly, uncertainty of the initial conditions (IC) has been evaluated from observation errors. Owing to local observations, uncertainty of the IC is small, except in the case of low cloud initialization.

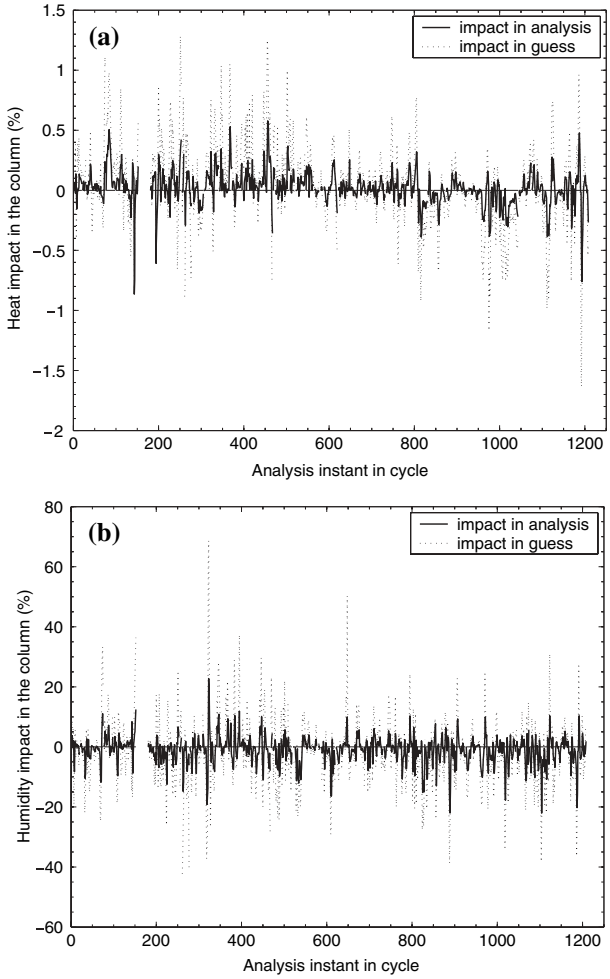

Figure 7
Advection contribution in heat (a) and humidity (b) balances for analysis and guess during the reference advection cycle for the winter season 2002–2003.

The impact of these incertainties for Cobel-Isba forecasts has been evaluated during a winter season. The study has shown the dependency between forecast time and dispersion (Fig. 9). IC uncertainties disperse during the first hours of the simulation (0 to 6 h), whereas the dispersion created by mesoscale forcing becomes more important in the second half of the simulation (6 to 12 h). The cloud radiative effect on dispersion is felt throughout the forecast period, as well as low cloud initialization. The heat and humidity budget analysis applied on the guess field has increased the understanding of the uncertainty influence on the COBEL-ISBA local forecast scheme. This strategy has permitted the quantification of the impact of perturbations on the variational data assimilation scheme. Perturbations grow

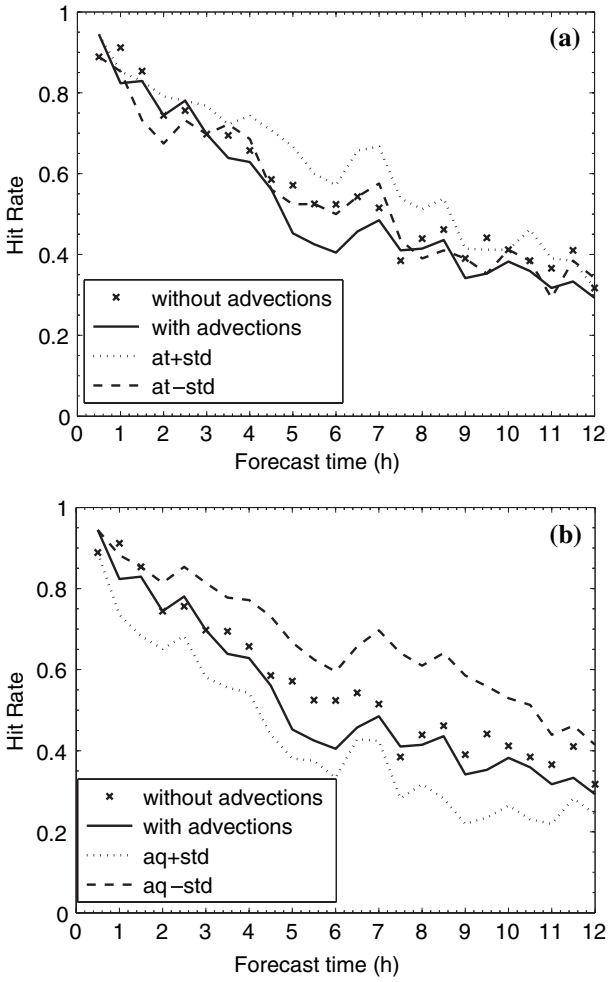

Figure 8
Hit rate for advection cycles for the winter season 2002–2003 (a). Hit rate comparisons of humidity advection cycles (b) for the winter season 2002–2003.

during the cycle and "feed" analyses through the assimination process. Each cycle evolves independently according to his perturbation.

One of the major avantages of a local approach (1-D) for short-term forecasts of fog and low clouds is that runs are "inexpensive". Within the perspective of a Local Ensemble Prediction System (L-EPS), this computational facility is highly advantageous in terms of computational time in an operational environment, and the freedom in the choice of the number of ensemble members is also a benefit. The study brings out interesting points for building a L-EPS, and they are listed below:

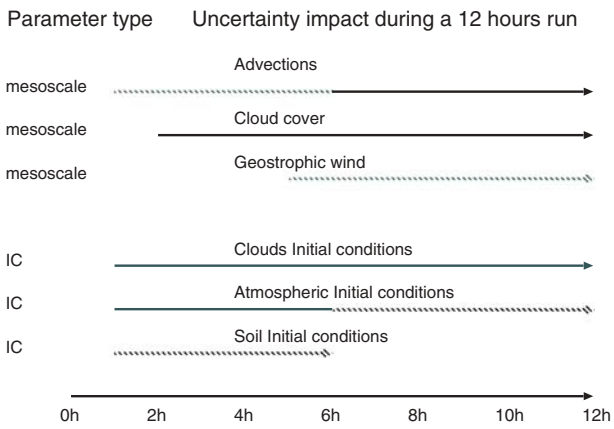

Figure 9
Summary of the uncertainty impact on fog and low cloud forecasts. For each parameter, the straight part of the arrows indicates when the dispersion is higher, the dashed part when dispersion is weaker during the 12 hour run.

- Construction of a L-EPS should take into consideration that dispersion is higher for mesoscale forcings compared to the IC. The sampling/calibration should be carefully done in order to balance both sources of uncertainty;
- construction of a L-EPS should also consider the dependency between run forecast time and dispersion. Sampling and calibration have to be carefully done for each forecast time;
- in this study the shape of uncertainty distribution has been evaluated, but not the magnitude. Consequently, a degree of freedom remains. This could be helpful to calibrate the dispersion of L-EPS;
- dissymetry (e.g., advection, atmospheric temperature profile) between perturbed cycles has been observed. Sampling/calibration have to be properly thought;
- a bias in the upper level of the atmospheric temperature profiles seems to affect the Cobel-Isba forecasts. The effect of this bias on the L-EPS should be studied in detail;
- perturbations could affect the forecasts through the assimilation system. Consequently, each member of L-EPS needs to have its own assimilation scheme.

All these points offer a starting point for building a L-EPS based on a COBEL-ISBA local numerical system. The COBEL-ISBA behavior has been determined during this study and results are encouraging.

References

Bergot, T. (1993), *Modélisation du brouillard à l'aide d'un modèle 1D forcé par des champs mésoéchelle: Application à la prévision*, Ph.D. Thesis - Université Paul Sabatier, Toulouse, France *1546*, 192 pp. (available at CNRM, Meteo-France).

Bergot, T. and Guédalia, D. (1994), *Numerical forecasting of radiation fog. Part I: Numerical model and sensitivity tests*, Mon. Wea. Rev. *122*, 1218–1230.

BERGOT, T., CARRER, D., NOILHAN, J., and BOUGEAULT, P. (2005), *Improved site-specific numerical prediction of fog and low clouds: A feasibility study*, Wea. Forecasting *20*, 627–646.

BOONE, A., MASSON, V., MEYERS, T., and NOILHAN, J. (2000), *The influence of the inclusion of soil freezing on simulations by a soil-vegetation-atmosphere transfer scheme*, J. Appl. Meteor. *9*, 1544–1569.

BOONE, A. (2000), *Modélisation des processus hydrologiques dans le schéma de surface ISBA: inclusion d'un réservoir hydrologique, du gel et la modélisation de la neige*, Ph.D. Thesis - Université Paul Sabatier, Toulouse, France.

BROWN, R. and ROACH, W.T. (1976), *The physics of radiation fog. Part II: A numerical study*, Quart. J. Meteor. Soc. *102*, 335–354.

CARRER, D. (2003), *Etude d'un système de prévision numérique locale des faibles visibilités sur Roissy. Final engineer formation repport n°860, ENM (Ecole Nationale de la Météorologie)* (available at Meteo-France/ENM, 42 Av Coriolis, F31057 Toulouse Cedex, France).

CLARK, D.A. (2002), *The 2001 demonstration of automated cloud forecast guidance products for San Francisco International airport*, 10th Conf. Aviation, Range and Aerospace Meteorology, AMS, Portland OR, May 13–16.

DUYNKERKE, P.G. (1991), *Radiation fog: A comparison of model simulation with detailed observations*, Mon. Wea. Rev. *119*, 324–341.

HERZEGH, P., PETTY, K., BENJAMIN, S., RASSMUSSEN, R., TSUI, T., WIENER, G., and ZWACK, P. (2002), *Development of automated national ceiling and visibility products: Scientific and pratical challenges, research strategies, and first steps*, 10th Conf. Aviation, Range, and Aerospace Meteorology, Am. Meteor. Soc.

JIUSTO, J.E. and LALA, G. (1983), *Radiation fog fields programs. Recents studies,* ASRC-SUNY Publication *117*, 67 pp.

KALNAY, E. (2003), *Atmospheric Modeling, Data Assimilation and Predictability* (Cambridge University Press, UK) 341 p.

MARZOUKI, H. (2005), *Impact d'un système d'assimilation dans un système de prévision numérique local des brouillards et des nuages bas, Final engineer formation report 1005, ENM (Ecole Nationale de la Météorologie)* (available at Meteo-France/ENM, 42 Av Coriolis, F31057 Toulouse, cedex, France).

MEYER, M.B., LALA, G.G., and JIUSTO, J.E. (1986), *Fog-82, A cooperative field study of radiation fog*, Bull. Am. Meteor. Soc. *67*, 825–832.

MUSSON-GUENON, L. (1987), *Numerical simulations of fog event with a one-dimensional boundary layer model*, Mon. Wea. Rev. *115*, 592–607.

ROQUELAURE, S. (2004), *Couplage du modèle COBEL avec le modèle de mésoéchelle RUC: advections horizontales de température et d'humidité*, M. Sc. Thesis - UQAM, Montréal, Canada, 113 pp.

TURTON, J.D. and BROWN, R. (1987), *A comparison of a numerical model of radiation fog with detailed observations*, Quart. J. Roy. Meteor. Soc. *113*, 37–54.

WALMSLEY, J., BURROWS, W.R., and SCHEMEAUER, R.S. (1999), *The use of routine weather observations to calculate liquid water content in summer high elevation fog*, J. Appl. Meteor. *38*, 369–384.

(Received April 11, 2006, accepted October 31, 2006)